Macromolecules

Article

pubs.acs.org/Macromolecules

Gas Transport Coefficients of Phthalide-Containing High-T_g Glassy Polymers Determined by Gas-Flux and NMR Measurements

Carolina García,[†] Ángel E. Lozano,[†,∥,⊥] José G. de la Campa,[†] Yakov Vygoskii,[‡] Mihail Zolotukhin,[§] Javier de Abajo,[†,∥] Leoncio Garrido,*[,†] and Julio Guzmán*[,†]

[†]Instituto de Ciencia y Tecnología de Polímeros, Consejo Superior de Investigaciones Científicas (ICTP-CSIC), Juan de la Cierva 3, 28006 Madrid, Spain

[‡]Nesmeyanov Institute of Organoelement Compounds, Russian Academy of Sciences, ul Vavilova 28, Moscow, 119991 Russia

[§]Instituto de Investigaciones en Materiales, Universidad Nacional Autónoma de México, Apartado Postal 70-360, CU, Coyoacán 04510 México City, D.F. México

[∥]Group of Porous Materials and Surfaces, UVa-CSIC Research Unit, SMAP, 47011 Valladolid, Spain

[⊥]IU CINQUIMA, Facultad de Ciencias, Universidad de Valladolid, E-47071 Valladolid, Spain

ABSTRACT: The synthesis of three aromatic polymers containing phthalide cardo groups having high inherent viscosities is described. Polyimides PIC-6F and PIC-TB were prepared from a cardo diamine and two different dianhydrides, and poly(phthalidylidenearylene) (PPDAr) was prepared by a precipitative Friedel–Crafts homopolycondensation of 3-(4-biphenylyl)-3-chlorophthalide. All polymers presented high glass transition temperatures varying between 600 and 690 K. Dense membranes prepared by casting from *N*,*N*-dimethylacetamide solutions exhibited good mechanical properties and decomposition temperatures over 770 K under a N_2 atmosphere. Results of gas transport measurements of O_2, N_2, and CO_2 were comparatively analyzed based on the chemical structure of the polymers. Additionally, the solubility, diffusion, and permeability coefficients of $[^{13}C]O_2$ in these membranes were determined by ^{13}C NMR spectroscopy and pulsed-field gradient NMR measurements, and the results were in good agreement with those determined with pressure-driven measurements. It was found that membranes of PPDAr exhibited the highest permeability and CO_2/N_2 and CO_2/O_2 permselectivities.

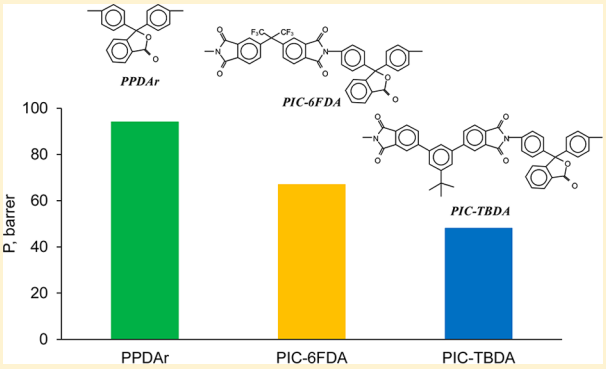

INTRODUCTION

Gas separation by polymer membranes is a growing field of application that is rapidly gaining technological importance. In fact, gas separation membranes are useful for a variety of industrial operations, such as nitrogen and oxygen enrichment, stripping of carbon dioxide from natural gas, hydrogen recovery from petrochemical recycling and purge gas streams, water vapor removal from air, recovering of volatile organic compounds and monomers, etc.[1−3] Unlike classical methods for gas separation and purification, membrane separation technologies have the advantages of energy efficiency, simplicity, and low cost. However, wider commercial utilization would still require the development of membranes with higher permeant fluxes and higher transport selectivity. The membranes currently used in most commercial applications are solution-diffusion membranes because transportation of gas molecules is mainly achieved by the solution and diffusion mechanism. The gas dissolves at the surface of the membrane and diffuses through by a series of activated steps. As the last step, the gas desorbs at the low-pressure side.

The solution-diffusion mechanism involves molecular scale interactions of the permeating gas with the polymer membrane; thus, it can be expressed in terms of the transport and sorption coefficients for the individual polymer and gas. A more common way of expressing this relation is

$$P = DS \tag{1}$$

The quantity *S*, solubility, is thermodynamic in nature and is affected by polymer−penetrant interactions as well as excess interchain gaps in glassy polymers, whereas the average diffusion coefficient, *D*, is kinetic in nature and determined mainly by the molecular size of the penetrant and polymer−penetrant dynamics.[4]

Significant progress in membrane separation technology depends on the explanation of the mechanism for gas transport. An insufficient understanding of the relationship between the chemical structure of a polymer and its gas transport properties

Received: January 27, 2015
Revised: March 31, 2015
Published: April 8, 2015

DOI: 10.1021/acs.macromol.5b00183
Macromolecules 2015, 48, 2585−2592

may hinder this progress. Because of the more restricted segmental motions in glassy polymers, these materials offer enhanced selectivity of gas components according to their diffusion characteristics as compared to rubbery polymers. An upper limit of performance for polymeric membranes has been noted for the industrially important separation of gas pairs, such as oxygen/nitrogen, hydrogen/methane, carbon dioxide/methane, or carbon dioxide/nitrogen. This observation was based on a comprehensive review of the gas transport properties of hundreds of commercial and experimental polymers. The conclusion was that in order to find new polymer materials that could eventually surpass the so-called Robeson upper limit, structural changes should be made, to control simultaneously polymer packing and rigidity. The best way to accomplish that seems to be a change in the primary chemical composition of the polymers, by introducing groups and moieties able to control both aspects.[5,6] Many attempts in this direction have already been made trying to properly combine the many factors related to the chemical structure of polymer affecting the membrane performance.[7−10]

It has been suggested that it is desirable to accomplish two aims simultaneously when varying the structure within a family of polymers: inhibit molecular packing while hindering the backbone mobility. The inhibition of molecular packing will increase the fractional free volume (FFV) of the polymer matrix, and this will translate into higher permeability. Hindering segmental mobility will lead to higher rigidity and higher glass transition temperatures (T_g), and these will turn to better selectivity. A number of studies have demonstrated that both permeability and permselectivity may be enhanced by incorporating bulky pendent groups in membrane-forming polymers, which simultaneously decrease chain packing efficiency and hinder torsional mobility. In this context, many data on structure−properties relationships have been reported for families of aromatic glassy polymers, such as polyamides,[11,12] polysulfones,[13−15] polycarbonates,[16,17] poly(aryl ether ketones),[18,19] polyimides,[20−23] and other polyheterocycles, including polymers of intrinsic microporosity (PIMs) and thermally rearranged polymers (TRs).[24−28]

The present study focuses on the effect of a systematic variation of the chemical structure on the gas permeability of three experimental aromatic polymers containing the phthalide moiety as a side group. Phthalide containing monomers are a class among the so-called cardo condensation monomers, and they were introduced at the beginning of the 1960s.[29] It has been shown that the presence of cardo groups in chains of different polymers hinders molecular attraction forces but at the same time greatly inhibits segmental mobility, with an overall result of rising the T_g and improving the solubility. Simultaneously, cardo groups in aromatic polymers twist the phenylene moieties of the main chain out of a planar conformation, thereby causing an increase in free volume. These characteristics make aromatic cardo polymers suitable candidates for gas separation applications.

Previous studies on gas membranes based on polymers containing cardo groups have shown that introducing these bulky monomers in polyesters,[30] polysulfones,[31] or poly(ether ketones)[32−34] greatly improved the permeation characteristics in comparison with those of analogous classical polymers.

The present report describes, for the first time, the synthesis of selected polyimides containing phthalide groups with the aim of obtaining polymer membranes having superior thermal resistance (service temperature approaching 300 °C) and mechanical behavior. The properties of these polymers are compared with those of previously reported polymers containing phthalide groups. Among these is poly[3,3-bis(4-phenylene)phthalide] (PPDAr), which has been newly synthesized for the present work and its permeation properties evaluated.

In addition, ^{13}C NMR spectroscopy and pulsed field gradient (PFG) NMR were used to determine all the gas transport coefficients and assess the appropriateness of the method by comparing the results with those attained by direct permeation measurements using the traditional barometric method.

EXPERIMENTAL PART

Materials. Starting reactants and commercially available solvents were used as received unless otherwise indicated. 2,2′-Hexafluoroisopropylidene diphthalic anhydride (6FDA, Chriskev, Kansas, USA) and anhydrous $AlCl_3$ (Sigma-Aldrich) were purified by sublimation. 5′-*tert*-Butyl-*m*-terphenyl-3,4,3″,4″-tetracarboxylic acid dianhydride (TBDA) was prepared in high yield (over 90%) by a synthetic method reported elsewhere[35] (mp 305 °C; lit. 304 °C).

Analysis for TBDA ($C_{26}H_{18}O_6$): Calcd C, 73.23; H, 4.25. Found: C, 73.00; H, 4.26. ^1H NMR (DMSO-d_6, ppm): 8.62 (d, 2H); 8.48 (dd, 2H); 8.16 (d, 2H,); 8.09 (t, 1H); 7.92 (d, 2H). ^{13}C NMR with proton decoupling (DMSO-d_6, ppm): 163.15; 163.01; 153.01; 147.88; 138.43; 135.04; 132.20; 129.86; 125.78; 125.23; 124.02.

The cardo diamine 3,3-bis(4-aminophenyl)isobenzofuran-1-(3*H*)-one (PHDA) was prepared and purified in accordance with a known procedure.[36,37] After recrystallization from ethanol, the melting point was 204−205 °C.

Analysis for PHDA ($C_{20}H_{16}N_2O_2$): Calcd C, 75.93; H, 5.10; N, 8.85. Found: C, 75.93; H, 5.39; N, 8.58.

The monomer 3-(4-biphenylyl)-3-chlorophthalide, **1**, was prepared by treatment of 2-(4-phenylbenzoyl)benzoic acid with an excess of thionyl chloride (mp 166.5−167.5 °C) according to the published method.[37]

Polymer Synthesis. *Polydiphenylene Phthalide Synthesis.* A 100 mL flask with reflux condenser was charged under a nitrogen atmosphere with 3.20 g of **1** (0.01 mol) and 50 mL of dichloroethane. To the obtained transparent solution, 1.86 g of $AlCl_3$ (0.014 mol) was added. The purple mixture was stirred rapidly for 12 h at room temperature. Afterward, the resulting suspension was filtered. Black particles on the filter were carefully washed with methanol, water, and acetone. The yield after drying in vacuum was 2.58 g (91%).

The reaction mass was dissolved in chloroform and precipitated in methanol; the precipitate was filtered off, washed with methanol and acetone, and dried at 120 °C.

Polyimide Synthesis. 5.0 mmol of diamine was dissolved in 20 mL of *m*-cresol in a 100 mL three-necked flask. 5.0 mmol of dianhydride was added, and the mixture warmed to 80 °C under a dry nitrogen atmosphere until total solution and then pyridine (0.3 mL) was added. The solution was maintained at that temperature for 1 h, and then benzoic acid (1 mmol) was added. The solution was heated to 190 °C, and the reaction proceeded for 6 h. After cooling, the very viscous solution was poured slowly into a mixture 1:2 (v/v) of water/ethanol, forming a white, fibrous precipitate that was filtered off, washed thoroughly with a mixture 1:1 (v/v) of water/ethanol, extracted with ethanol in a Soxhlet apparatus, and dried in a vacuum oven at 100 °C overnight. The yields were nearly quantitative.

Polymer Characterization. Inherent viscosities were determined at 25 °C with an Ubbelohde viscometer using *N*-methyl-2-pyrrolidinone (NMP) as a solvent with 0.5 g/dL polymer solutions. ^1H and ^{13}C with proton decoupling NMR spectra were recorded on a Varian Innova 300 spectrometer operating at ^1H and ^{13}C Larmor frequencies of 300 and 75.43 MHz, respectively. Fourier transform infrared (FT-IR) spectra were obtained on a PerkinElmer RX-1 FT-IR spectrometer, fitted with an ATR dispositive. Qualitative solubility was determined using 10 mg of polymer in 1 mL of solvent at room temperature. Samples that did not dissolve after stirring at room temperature for 24 h were heated up to the boiling temperature of the solvent.

DOI: 10.1021/acs.macromol.5b00183
Macromolecules 2015, 48, 2585−2592

Differential scanning calorimetry (DSC) analyses were performed on a PerkinElmer DSC7 calorimeter at a heating rate of 20 K/min under nitrogen. Thermogravimetric analyses (TGA) were performed on a TA Instruments Q500 thermobalance heating at 10 K/min under controlled flux of nitrogen (60 mL/min). Wide-angle X-ray scattering difractograms were performed at room temperature on a Bruker D8 Advance system provided with a Vantec 1 detector, using radiation Cu Kα of 1.54 Å at 40 kV/40 mA.

Polymer density was measured on films by the flotation method. The density data were used to evaluate chain packing by calculating the fractional free volume (FFV) using the relation

$$\mathrm{FFV} = (V - 1.3V_w)/V \quad (2)$$

where V is the polymer specific volume and V_w is the specific van der Waals volume. The van der Waals volume was estimated by several approximations, including the traditional method of Bondi[38] and the Hyperchem computer program,[39] version 7.51. Hyperchem employs a grid method based on the work of Bodor et al.,[40] using the atomic radii supplied by Gavezotti.[41] Moreover, the computer-based method can estimate van der Waals volume for structural units not included in the tables typically used by the Bondi method.

Film Preparation. Membranes were prepared by casting a 6−8% (w/v) solution in *N*,*N*-dimethylacetamide (DMA) on a balanced glass plate fixed to a heating plate. The films were dried at 80 °C/24 h, stripped off from the glass plate, and treated in a vacuum oven at 180 °C for 24 h and then 6 h at 250 °C, both under vacuum. As a result, a negligible amount of solvent remained, as confirmed by thermogravimetric analysis (TGA).

Permeation Measurements. A laboratory-made permeator, described elsewhere,[42] was used for permeation measurements. Briefly, it consists of a gas cell in which the polymer membrane is placed in the center, separating the high-pressure or upstream chamber from the low-pressure or downstream chamber. High vacuum was generated in the permeation device by means of an Edwards molecular turbo-pump to reaching a low pressure of about 10^{-6} bar, and the whole arrangement was thermostatically controlled at 30 °C by means of a water bath. Subsequently, the gas contained in the high pressure chamber was allowed to flow into the downstream chamber, and the evolution of the pressure of the gas in this chamber was monitored with a MKS Baratron type 627B absolute pressure transducer working in the pressure range 10^{-4}−1 mmHg. Pressure in the upstream chamber was measured with a Gometrics transducer and was varied between 0.1 and 5 bar in this work. Three independent experiments were undertaken for each membrane and gas.

The permeability and diffusivity coefficients were calculated from the curves measuring the pressure increase at the downstream side, recorded at intervals of 1 s.

The tested gases employed in the transport measurements, all with purity higher than 99%, were nitrogen, oxygen, and carbon dioxide.

Solubility and Diffusion Measurements by ^{13}C NMR. Membrane strips less than 2 mm wide and approximately 1 cm long were placed inside a 10 mm o.d. NMR tube designed for NMR studies of moderately pressurized gases. In addition, a standard consisting of a sealed glass capillary with a known amount of [^{13}C(1)] labeled (99.9%, Euriso-top, Gif-sur-Yvette, France) acetic acid was placed in the tube. Prior to filling the tube at a given pressure with [^{13}C]O_2 (99%, Cambridge Isotopes Laboratories, Andover, MA) or nonlabeled CO_2, the air was removed by vacuum. Unless indicated otherwise, the gas pressure used in these experiments was in the range of 2−5 bar to facilitate the measurements with adequate signal-to-noise ratio in a reasonable amount of time. The gas pressure was monitored with a transducer working in the range 0−10 bar. The diffusion coefficient of the gas in the membranes was estimated by a spin-echo type of radio-frequency (rf) pulse sequence, as shown by Stejskal et al.[43] The measurements were performed on a Bruker Avance 400 spectrometer equipped with a 89 mm wide bore and a 9.4 T superconducting magnet (^{13}C Larmor frequency at 100.61 MHz). The reported data were acquired at 30 ± 0.5 °C with a Bruker diffusion probe head (Diff60) using 90° ^{13}C rf pulse length of about 12 μs. An inversion−recovery pulse sequence was used to estimate the ^{13}C longitudinal relaxation times, T_1, of sorbed gas. Solubility measurements were performed by acquiring ^{13}C NMR spectra of samples using a single pulse excitation sequence with a repetition rate of 14 s. For diffusion measurements, a pulsed field gradient stimulated spin echo pulse sequence was used. The echo time between the first two 90° rf pulses, τ_1, was 2.11 ms. The apparent diffusion coefficient of [^{13}C]O_2, D, was measured at diffusion times, Δ, of 240 ms. The length of the field gradient pulses, δ, was 1 ms, and the amplitude of the gradient pulses, g, varied from 1.7 up to a maximum value of 20 T m^{-1}. The repetition rate was 14 s. The total acquisition time for these experiments ranged from 3.5 to 87 h. Self-diffusion coefficients may be calculated by fitting the experimental data to the corresponding exponential function,[43] but, as it will be shown later, two decreasing exponential functions were used. This approach allows the calculation of two diffusion coefficients that represent more adequately the behavior of glassy polymer membranes.

All ^{13}C NMR spectra were referenced to [^{13}C(1)] acetic acid (178.1 ppm), secondary to tetramethylsilane (0.0 ppm).

Previous to these measurements, the field gradient was calibrated following the spectrometer manufacturer's protocol at 25 ± 0.5 °C, using a sample of water doped with $CuSO_4$ at 1.0 g/L and a value of the water diffusion coefficient equal to 2.3×10^{-5} cm^2/s. Furthermore, the calibration was verified at the range of gradient values used experimentally by measuring the diffusion coefficient of dry glycerol. A value of $D = 2.23 \times 10^{-8}$ cm^2/s was found, in good agreement with the results reported for this parameter elsewhere.[44] Also, diffusion measurements for these two liquids were performed over a wide range of diffusion times to assess the stability of the gradients and whether artifacts due to eddy (Foucault) currents could affect the measurements. The temperature at the sample volume in the probe head was determined by measuring the difference between the proton chemical shifts of a solution of ethylene glycol at 80% v/v in deuterated dimethyl sulfoxide.

With the experimental system indicated above and by using the internal standard concentration, it was possible to determine both the solubility and diffusion coefficients of the gas in the polyimide membranes and, consequently, the corresponding permeability coefficients.

RESULTS AND DISCUSSION

Polymer Preparation and Characterization. Noncommercial monomers were prepared for this work following the synthetic routes previously outlined by the authors.[36,37] Thus, 5-*tert*-Butyl-*m*-terphenyltetracarboxylic acid dianhydride (TBDA) was synthesized by an improved, high yield method starting from 3,5-dibromo-5-*tert*-butylbenzene and 3,4-dimethylphenylboronic acid. 1-Oxo-3,3-bis(4-aminophenyl)dihydrobenzofuran (PHDA) was prepared by Friedel−Crafts condensation of phthaloyl chloride and carbanilide promoted by $AlCl_3$, with subsequent hydrolysis in the presence of acid (H_2SO_4) for PHDA. Commercial and noncommercial monomers could be conveniently purified by recrystallization from suitable solvents to polycondensation grade.

Polyimide synthesis was accomplished by the method of high-temperature one-step polyimidation in *m*-cresol solution. Using this method, two polyimides containing cardo groups were prepared and isolated in virtually quantitative yield.

Poly(phthalidylidenearylene) (PPDAr) was prepared by a precipitative Friedel−Crafts homopolycondensation of 3-(4-biphenylil)-3-chlorophthalide. The preparation of polymers performed by precipitative electrophilic polycondensation allows the synthesis of high molecular weight polymers in particle form. To carry out a precipitative homopolycondensation of PPDAr, the same reaction conditions described in the precipitative polyketone synthesis frequently reported (dichloroethane as a solvent, $AlCl_3$ as catalyst, and room temperature) were used.[45] The yield of PPDAr synthesis was 90%.

DOI: 10.1021/acs.macromol.5b00183
Macromolecules 2015, 48, 2585−2592

All the three polymers were purified and subjected to the common identification techniques. The chemical structures of the repeating units are given in Scheme 1.

Scheme 1. Repeating Unit of Polymers

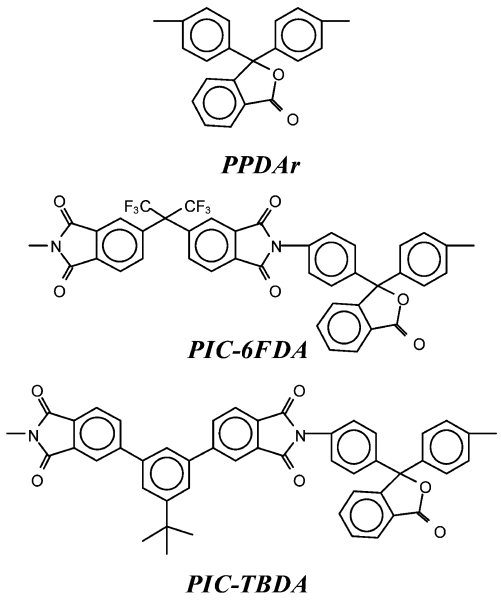

The two polyimides, PIC-6FDA and PIC-TBDA, were soluble in organic aprotic solvents such as DMA, NMP, or DMSO, while PPDAr was soluble also in common solvents like chloroform. Nonetheless, polymer films were prepared by casting from DMA solutions in all cases. Inherent viscosities in the range 0.46−0.85 dL/g indicated high molecular weight for these polymers, and this assumption is in agreement with the excellent mechanical properties exhibited by all materials (tensile strength over 80 MPa and modulus over 2.7 GPa).

The composition of these polymers was determined by elemental analysis, FT-IR spectroscopy, and NMR spectroscopy. As an example, the FT-IR spectrum of polymer PIC-6FDA is shown in Figure 1. The most characteristic absorption bands appeared at 1774 and 1719 cm^{-1}, attributable to symmetric and asymmetric stretching of imide carbonyls, as well as a strong, sharp band around 725 cm^{-1} (peak at 713 cm^{-1}) associated with skeletal vibration of the imide ring, which overlaps with the stretching vibration of C−F bonds. The carbonyl C═O band of the cyclic lactone, which should appear at about 1710 cm^{-1}, is overlapped with the imide band of 1719 cm^{-1}. The band at 1365 cm^{-1} could be attributed to the C−N−C stretching. Figure 2 illustrates the ^{1}H NMR and ^{13}C with proton decoupling NMR spectra of polymer PIC-6FDA, where all the signals could be assigned readily to the protons and carbons of the polymer.

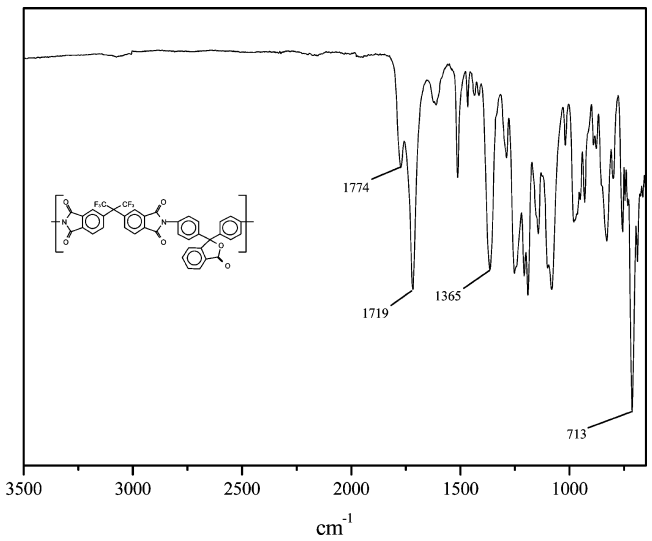

Figure 1. FT-IR spectrum of polymer PIC-6FDA.

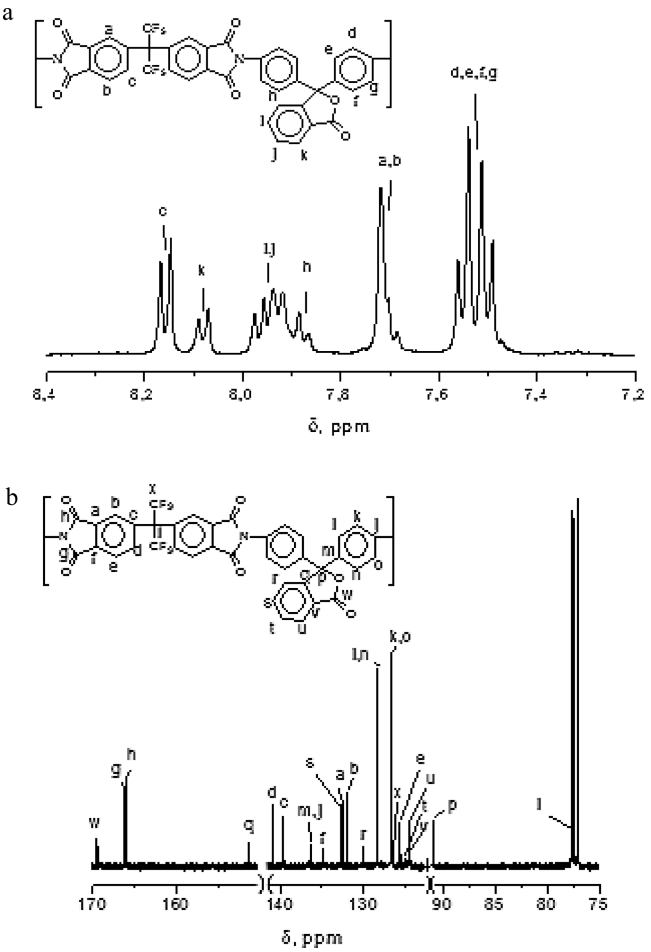

Figure 2. (a) ^{1}H NMR ($CDCl_3$, ppm): 7.52 (dd 4H); 7.70 (m 2H); 7.87 (d 1H); 7.92 (dd 1H); 7.97 (dd 1H); 8.08 (d 1H); 8.16 (d 1H). (b) ^{13}C with proton decoupling NMR ($CDCl_3$, ppm): 169.4 (C_w); 166.1 (C_g); 165.9 (C_h); 151.2 (C_q); 140.7 (C_d); 139.5 (C_c); 136.3 (C_m y C_j); 132.7 (C_s); 134.4 (C_a); 131.9 (C_b); 130.1 (C_r); 128.3 (C_l y C_n) 126.6 (C_k y C_o); 126.5 (C_x); 125.6 (C_e); 125.0 (C_t); 124.5 (C_u); 124.4 (C_v); 90.8 (C_p); 77.5 (C_i).

Glass transition (T_g) and initial decomposition (T_d) temperatures were determined by DSC and by TGA, respectively. DSC curves, recorded from 323 to 703 K, showed only one inflection, which was attributed to the T_g. No exotherm or endotherm peaks, indicative of crystallization or melting, were detected in any case. T_g values ranging from 603 to 683 K were measured (Table 1). Decomposition temperatures (taken as the temperature of the initial weight loss onset in the TGA curves) were above 770 K for all of the polymers, as it could be expected for aromatic polymers. The values of T_g and T_d determined for PPDAr were similar to those found previously.[46]

DOI: 10.1021/acs.macromol.5b00183
Macromolecules 2015, 48, 2585−2592

Table 1. Inherent Viscosities, Specific Volumes, Glass Transition Temperatures, Thermal Degradation Temperatures, and Fractional Free Volume of Polymer Membranes

polymer	η_{inh}, dL/g	V, cm^3/g	T_g, K	T_d, K	FFV
PPDAr	0.81	0.827	683	773	0.182
PIC-6FDA	0.46	0.736	603	805	0.214
PIC-TBDA	0.85	0.819	659	779	0.171

Permeability, Diffusion, and Solubility Coefficients. To determine the transport coefficients of the membranes, several measurements of the gas flux through the polyimide membranes were performed using the pressure device described in the Experimental Part. The time dependence of the gas pressure in the downstream chamber is calculated by the integration of Fick's second law, and with appropriate boundary conditions, one obtains when steady-state conditions are reached that the time dependence of the pressure of the downstream chamber can be written as[47,48]

$$p(t) = 0.2786\frac{pALST}{V}\left(\frac{Dt}{L^2} - \frac{1}{6}\right) \quad (3)$$

In this equation, $p(t)$ and p, which denote the pressures of gas in the downstream and upstream chambers, respectively, are given in cmHg, A and L represent the area and thickness of the membrane in cm^2 and cm, respectively, V the volume of the downstream chamber in cm^3, and D and S are the diffusion and solubility coefficients in cm^2/s and cm^3 gas (STP)/(cm^3 polymer cmHg), respectively.

As an example, illustrative plots of the variation of pressure with time in the downstream chamber for the permeation of CO_2 in a polymer membrane of PPDAr are shown in Figure 3.

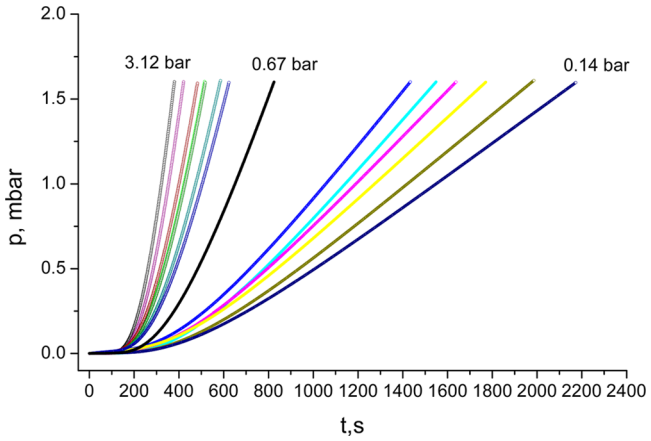

Figure 3. Variation of pressure in the downstream chamber for the permeation of CO_2 in a membrane of PPDAr, thickness of 90 μm, at pressures in the upstream chamber between 0.14 and 3.12 bar (the low, intermediate, and high values are indicated).

These plots in the steady state are straight lines intercepting the abscissa axis at

$$D = \frac{L^2}{6\theta} \quad (4)$$

where θ is the time lag and, therefore, the diffusion coefficient can be obtained from eq 4. Assuming that the permeability coefficient, P, is the product of the solubility coefficient and the diffusion coefficient, the value of P in barrer (1 barrer [10^{-10} cm^3(STP) cm/(cm^2 s cmHg)]) could be obtained from eq 5

$$P = 3.59\frac{VL}{pAT}\lim_{t\to\infty}\left(\frac{dp(t)}{dt}\right) = \frac{\Omega}{p} \quad (5)$$

where $\lim_{t\to\infty}(dp(t)/dt)$ is the stationary flux in the downstream chamber and $\Omega = 3.59(VL/AT)\lim_{t\to\infty}(dp(t)/dt)$. In Figure 4,

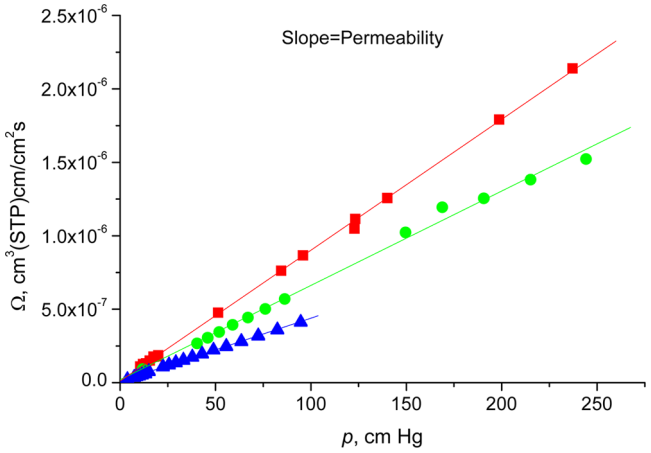

Figure 4. Ω vs p (gas pressure) for CO_2 (red squares), oxygen (green circles), and nitrogen (blue triangles) on PPDAr at 30 °C.

graphs corresponding to the permeation experiments of CO_2, N_2, and O_2 on PPDAr performed at different pressures and expressed in the form of Ω vs p are depicted. It can be seen that straight lines are obtained, and from their slopes the values of the permeability are calculated. The obtained straight lines indicate that, in the range of pressures studied, the permeability is constant, and similar results were obtained for the other gases studied: oxygen and nitrogen.

Once the permeability and diffusion coefficients are determined, the solubility coefficients can be calculated directly from the P/D ratio, and the results obtained for the transport coefficients of the gases in the three polymers are shown in Tables 2 and 3.

The comparative analysis of the transport coefficients of the three polymers clearly indicates that the highest permeability to CO_2 corresponds to membranes of PPDAr with a value of 94 barrer while membranes PIC-6FDA and PIC-TBDA showed values of 67 and 48 barrer, respectively. This behavior could be attributed to the higher fraction of nonequilibrium excess free volume in the glassy state for the PPDAr membranes that permits higher gas adsorption in the Langmuir sites and consequently higher solubility coefficients in the case of more condensable gases, such as CO_2.

On the contrary, the permeabilities to oxygen of the three membranes are almost the same, which is the origin of the high permselectivity of membrane PPDAr as is shown in Table 3. Concerning the permeability to nitrogen, the variation is between 2.0 and 2.5 barrer, with the lower and higher values corresponding to the PIC-TBDA and PPDAr, respectively.

Recently, we have described[49] the application of NMR spectroscopy to the determination of all the three gas transport coefficients through liquids and polymers. In the following, we describe the use of this technique to determine the solubility, diffusion, and permeability coefficients of [^{13}C]O_2 in the membranes described in this work.

DOI: 10.1021/acs.macromol.5b00183
Macromolecules 2015, 48, 2585−2592

Table 2. Permeability, Diffusion, and Solubility Coefficients of Carbon Dioxide in Membranes at 30 °C, Measured with the Pressure and NMR Methods

membrane	method	p, bar	P, barrer	$D \times 10^8$, cm^2/s	S, cm^3 (STP)/(cm^3 cmHg)
PPDAr	pressure	0−3.2	94 ± 2	2.5−3.5	0.40−0.25
	NMR (CO_2)	4.06			0.185
	NMR ($[^{13}C]O_2$)	1.73−4.24	91 ± 6	4.0−5.3	0.23−0.16
PIC-6FDA	pressure	0−4.7	67 ± 3	1.26−2.1	0.62−0.31
	NMR (CO_2)	3.96			0.218
	NMR ($[^{13}C]O_2$)	1.66−4.07	63 ± 10	2.2−2.8	0.32−0.19
PIC-TBDA	pressure	0−5.3	48 ± 2	3−4.2	0.15−0.12
	NMR (CO_2)	4.12			0.169
	NMR ($[^{13}C]O_2$)	1.54−4.02	45 ± 7	2.0−2.8	0.24−0.15

Table 3. Permeability and Diffusion Coefficients of O_2, N_2, and CO_2 and CO_2/O_2 and CO_2/N_2 Permselectivities in Cardo Polymer Membranes at 30 °C and 1 bar

membrane	P_{O_2}, barrer	P_{N_2}, barrer	P_{CO_2}, barrer	$D_{O_2} \times 10^8$, cm^2/s	$D_{N_2} \times 10^8$, cm^2/s	$D_{CO_2} \times 10^8$, cm^2/s	α (CO_2/O_2)	α (CO_2/N_2)
PPDAr	11.8	2.5	94	7.74	2.7	2.6	7.97	37.6
PIC-6FDA	11.6	2.2	67	5.04	1.27	1.4	5.77	30.5
PIC-TBDA	10.0	2.0	48	5.67	1.42	3.1	4.8	24

The ^{13}C NMR spectra of these type of samples with the standard labeled $^{13}C(1)$ acetic acid showed three peaks as illustrated in earlier work:[49] one peak corresponding to the ^{13}C signal of the carboxyl group of acetic acid at 178.1 ppm and two peaks associated with the $[^{13}C]O_2$ in the membranes, centered at 128.4 and 125.6 ppm.[49] These two peaks reflect the existence of two populations of $[^{13}C]O_2$ corresponding respectively to the nonsorbed (free) and sorbed (in the membrane) gas fractions, in a slow exchange regime. The estimated spin−lattice relaxation times, T_1, of sorbed gas in the membranes were ∼2.3 s. The free gas exhibits T_1 values in the range of 50−65 ms.

After reaching equilibrium conditions, the solubility of $[^{13}C]O_2$ in the membranes was determined by comparing the areas of the peaks associated with the reference compound (acetic acid) and the sorbed gas in the corresponding ^{13}C NMR spectra. The results are comparatively analyzed with those obtained by permeation measurements as it is shown in Figure 5 for the solubility of CO_2 and $[^{13}C]O_2$ in PPDAr membranes, and all the results are summarized in Table 2.

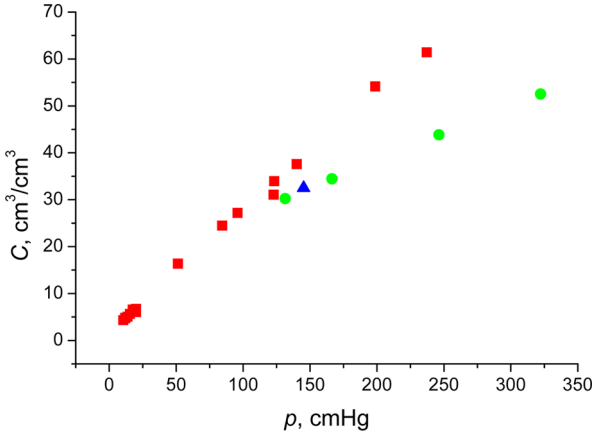

Figure 5. Variation of the concentration of CO_2 in a membrane of PPDAr as indirectly measured by pressure method (red squares) and directly measured ($[^{13}C]O_2$, NMR method) (green circles). The blue triangle corresponds to a measure by NMR with unlabeled CO_2.

In Figure 5, it can be seen that the solubility coefficients of $[^{13}C]O_2$ and CO_2 measured by NMR at low pressures are similar to those determined by permeation experiments, whereas at relatively high pressures, some differences occur. This could be due to the high rate of permeation observed for CO_2 (see Figure 3) in the barometric measurements that precludes an accurate determination of the diffusion and solubility coefficients, although the permeability coefficients can be accurately determined even at high pressures. In this regard, the measurement of D and S with the NMR method, at equilibrium, could be less prone to uncertainties in membranes exhibiting high permeability.

The diffusion coefficient of CO_2 in the membranes was also measured with NMR. For illustrative purposes, ^{13}C PFG NMR spectra corresponding to $[^{13}C]O_2$ sorbed in PPDAr, at p of 3.24 bar, are shown as a function of the amplitude of the field gradient in Figure 6.

For diffusion in liquid media or in nonglassy polymer membranes, the echo attenuation can be written as[43]

$$A(g) = A(0)\exp[-(b_{NMR}D)] \quad (6)$$

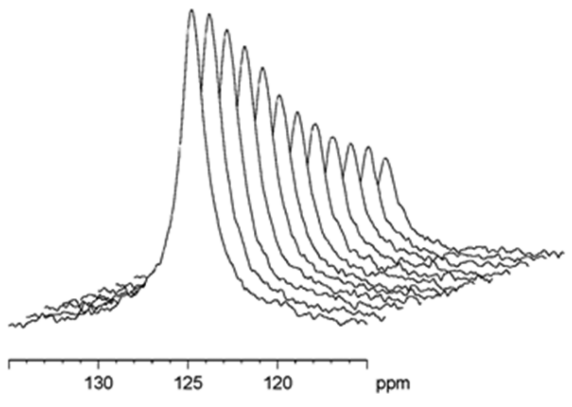

Figure 6. ^{13}C PFG NMR spectra corresponding to $[^{13}C]O_2$ sorbed in PPDAr obtained at 30 °C and a gas pressure of 3.24 bar. The duration, δ, of the gradient pulse was 1 ms, and the diffusion time, Δ, was 240 ms. The gradient amplitude, g, was incremented in 12 consecutive steps of 1.70 T/m from an initial value of 1.70 T/m.

DOI: 10.1021/acs.macromol.5b00183
Macromolecules 2015, 48, 2585−2592

where $A(g)$ and $A(0)$ are the amplitude of the echo in the presence of a gradient pulse with amplitude g and 0, respectively, $b_{NMR} = (\gamma g \delta)^2(\Delta - \delta/3)$ where γ is the gyromagnetic ratio of the nucleus being observed, and the others as previously defined. Figure 7 illustrates the attenuation of the echo intensity with

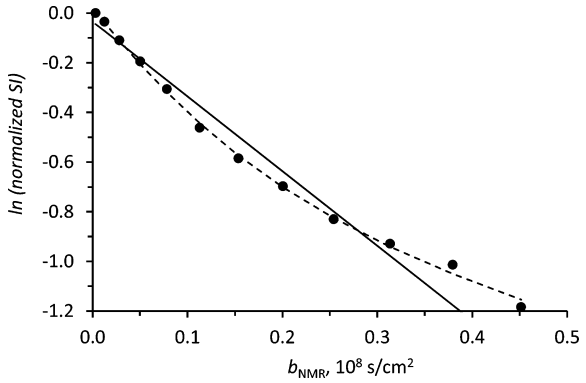

Figure 7. Plot of the normalized echo intensities vs the field gradient parameter b_{NMR} corresponding to a membrane of PPDAr loaded with $[^{13}C]O_2$ at 3.24 bar and 30 °C. The closed circles represent the experimental data points, and the solid and dashed lines represent the fits to eqs 6 and 9, respectively.

increasing values of b_{NMR}, keeping Δ and δ constant, corresponding to data shown in Figure 6. It is clearly shown that the data does not fit a monoexponential decay (eq 6).

As it is well established, the sorption isotherms in glassy polymer membranes are well described by the dual model that assumes two coexistent phases: one continuous where the sorption process obeys Henry's behavior and another discrete with Langmuir adsorption sites. In this model the solubility coefficient S is dependent on the gas pressure p in the form[50,51]

$$S = k_D + \frac{C'_H b}{1 + bp} \tag{7}$$

where k_D is Henry's constant, C'_H is the concentration of gas in Langmuir sites, and b is an affinity gas−polymer parameter.

Therefore, the permeability of the membrane is described by the equation

$$P = k_D D_D + \frac{C'_H b}{1 + bp} D_H \tag{8}$$

where D_D and D_H are respectively the diffusion coefficients in the continuous phase and Langmuir sites. This equation is really a simplified approach because the coupling between both diffusion modes is neglected.[52]

Thus, considering the dual model with two diffusion coefficients, the NMR diffusion data were analyzed using the sum of two decreasing exponentials according to a modification of eq 6 in the form

$$A(g) = A(0)[\varphi \exp(-b_{NMR} D_D) + (1 - \varphi) \exp(-b_{NMR} D_H)] \tag{9}$$

where φ is the fraction of gas in the continuous phase and $(1 - \varphi)$ represents the corresponding fraction in the Langmuir sites. Table 4 summarizes the diffusion coefficients determined in this manner at various pressures for all membranes. It is observed that D_D and D_H differ by about 1 order of magnitude. The permeabilities are then determined using the equation

Table 4. Summary of Results Obtained by NMR Spectroscopy and PFG NMR for the Transport Coefficients of $[^{13}C]O_2$ in Cardo Polymer Membranes at 30 °C

sample	p, bar	S, cm^3 STP/(cm^3 cmHg)	$D_D \times 10^8$, cm^2/s	φ	$D_H \times 10^8$, cm^2/s	P, barrer	$D_M \times 10^8$, cm^2/s
PPDAr	1.73	0.230	9.9	0.31	1.3	91	3.97
	2.19	0.207	11.1	0.36	1.2	99	4.76
	3.24	0.178	8.5	0.51	1.1	87	4.87
	4.24	0.163	8.4	0.57	1.1	86	5.26
PIC-6FDA	1.66	0.318	8.2	0.23	0.36	69	2.16
	2.28	0.275	10.8	0.19	0.74	73	2.65
	3.26	0.202	8.7	0.27	0.56	56	2.76
	4.07	0.193	9.1	0.22	1.0	54	2.78
PIC-TBDA	1.54	0.237	18.7	0.05	1.1	47	1.98
	2.42	0.188	11.7	0.19	0.64	52	2.74
	2.96	0.169	14.4	0.13	1.1	48	2.83
	4.02	0.145	5.9	0.34	0.60	35	2.40

$$P = S[\varphi D_D + (1 - \varphi) D_H] \tag{10}$$

With the values of permeability thus obtained and the solubility coefficients, we also obtain a mean diffusion coefficient D_M that should be equivalent to that determined by barometric measurements. The values of D_M are shown in Table 4. A fair agreement is observed between the results obtained by both procedures for all the transport coefficients (see Table 2), which clearly indicate the appropriateness of the NMR method to the determination of gas transport in glassy membranes. Moreover, this method offers the possibility of measuring D and S of each component in a gas mixture, providing that the gas molecules have an NMR observable nucleus and the corresponding NMR spectrum is resolved.

CONCLUSIONS

Two polyimides have been newly prepared that are soluble in organic solvents and easily processable into films with good mechanical and thermal properties. The behavior of these polyimides was compared with that of a polymer [poly(phthalidylidenearylene), PPDAr] synthesized by an electrophilic reaction and formed through the direct condensation of a precursor derived from phthalic anhydride and biphenyl. It was found that all polymers showed excellent thermal properties, but the values of the transport properties of the polyimides were lower than those of PPDAr.

The solubility and diffusion coefficients of C-13-labeled carbon dioxide were determined with NMR methods. The NMR diffusion measurements were adequately described by a dual model, and the transport coefficients determined were in good agreement with those obtained by the permeation method. The results support the suitability of the NMR method to measure the transport coefficients of gases in glassy polymer membranes.

AUTHOR INFORMATION

Corresponding Authors

*Tel +34 91 262 2900; Fax +34 91 564 4853; e-mail lgarrido@cetef.csic.es (L.G.).

*Tel +34 91 262 2900; Fax +34 91 564 4853; e-mail jguzman@ictp.csic.es (J.G.).

Notes

The authors declare no competing financial interest.

DOI: 10.1021/acs.macromol.5b00183
Macromolecules 2015, 48, 2585−2592

■ ACKNOWLEDGMENTS

The financial support of this work by the Spanish Ministry of Economy and Competitiveness (MAT2010-20668, MAT2013-45071-R, and MAT 2011-29174-C02-02) and the Consejo Superior de Investigaciones Científicas (CSIC) is greatly appreciated.

■ REFERENCES

(1) Bernardo, P.; Drioli, E.; Golemme, G. *Ind. Eng. Chem. Res.* **2009**, *48*, 4638−4663.
(2) Sanders, D. F.; Smith, Z. P.; Guo, R.; Robeson, L. M.; McGrath, J. E.; Paul, D. R.; Freeman, B. D. *Polymer* **2013**, *54*, 4729−4761.
(3) Yampolskii, Y. *Macromolecules* **2012**, *45*, 3298−3311.
(4) Yampolskii, Y., Pinau, I., Freeman, B. D., Eds.; *Materials Science of Membranes for Gas and Vapor Separation*; Wiley: Chichester, West Sussex, UK, 2006.
(5) Robeson, L. M. *J. Membr. Sci.* **1991**, *62*, 165−185. Robeson, L. M. *J. Membr. Sci.* **2008**, *320*, 390−400.
(6) Freeman, B. D. *Macromolecules* **1999**, *32*, 375−380.
(7) Robeson, L. M.; Burgoyne, W.; Langsam, F. M.; Savoca, A. C.; Tien, C. F. *Polymer* **1994**, *35*, 4970−4978.
(8) de Abajo, J.; de la Campa, J. G.; Lozano, A. E.; Espeso, J.; García, C. *Macromol. Symp.* **2003**, *199*, 293−305.
(9) Bas, C.; Mercier, R.; Sánchez-Marcano, J.; Neyertz, S.; Alberola, N.; Pinel, D. E. *J. Polym. Sci., Part B: Polym. Phys.* **2005**, *43*, 2413−2426.
(10) Maya, E. M.; García-Yoldi, I.; Lozano, A. E.; de la Campa, J. G.; de Abajo, J. *Macromolecules* **2011**, *44*, 2780−2790.
(11) Morisato, A.; Ghosal, K.; Freeman, B. D.; Chern, R. T.; Alvarez, J. C.; de la Campa, J. G.; Lozano, A. E.; de Abajo, J. *J. Membr. Sci.* **1995**, *104*, 231−241.
(12) Espeso, J.; Lozano, A. E.; de la Campa, J. G.; de Abajo, J. *J. Membr. Sci.* **2006**, *280*, 659−665.
(13) Aguilar-Vega, M.; Paul, D. R. *J. Polym. Sci., Part B: Polym. Phys.* **1993**, *31*, 1599−1610.
(14) Kim, H. J.; Hong, S. I. *Korean J. Chem. Eng.* **2000**, *17*, 122−127.
(15) Lee, K. J.; Jho, J. Y.; Kang, Y. S.; Won, J.; Gai, Y. D.; Robertson, G. P.; Guiver, M. D. *J. Membr. Sci.* **2003**, *223*, 1−10.
(16) Muruganandam, N.; Paul, D. R. *J. Membr. Sci.* **1987**, *34*, 185−198.
(17) Sen, D.; Kalipcilar, H.; Yilmaz, L. *Sep. Sci. Technol.* **2006**, *41*, 1813−1828.
(18) Wang, Z.; Chen, T.; Xu, J. *Macromolecules* **2000**, *33*, 5672−5679.
(19) García, C.; Tiemblo, P.; Lozano, A. E.; de Abajo, J.; de la Campa, J. G. *J. Membr. Sci.* **2002**, *205*, 73−81.
(20) Tanaka, K.; Kita, H.; Okano, M.; Okamoto, K. *Polymer* **1992**, *33*, 585−592.
(21) Wind, J. D.; Staudt-Bickel, C.; Paul, D. R.; Koros, W. J. *Macromolecules* **2003**, *36*, 1882−1888.
(22) Stern, A.; Liu, Y.; Feld, W. A. *J. Polym. Sci., Part B: Polym. Phys.* **1993**, *31*, 939−951.
(23) Calle, M.; Lozano, A. E.; de Abajo, J.; de la Campa, J. C.; Alvarez, C. *J. Membr. Sci.* **2010**, *365*, 145−153.
(24) Kumbharkar, S. C.; Karadkar, P. B.; Kharul, U. K. *J. Membr. Sci.* **2006**, *286*, 161−169.
(25) Bai, H.; Ho, W. S. W. *Ind. Eng. Chem. Res.* **2009**, *48*, 2344−2354.
(26) Tejero, R.; Lozano, A. E.; Alvarez, C.; de Abajo, J. *J. Polym. Sci., Part A: Polym. Chem.* **2013**, *51*, 4052−4060.
(27) Budd, P. M.; McKeown, N. B. *Polym. Chem.* **2010**, *1*, 63−68.
(28) Kim, S.; Lee, Y. M. *Prog. Polym. Sci.* **2014**, DOI: 10.1016/j.progpolymsci.2014.10.005.
(29) Korshak, V. V.; Vinogradova, S. V.; Vygodskii, Y. S. *J. Macromol. Sci., Rev. Macromol. Chem.* **1974**, *C11*, 45−142.
(30) Sheu, F. R.; Chern, R. T. *J. Polym. Sci., Part B: Polym. Phys.* **1989**, *27*, 1121−1133.
(31) Oude, A. Y.; Kulkarni, S. S.; Kulkarni, M. G. *J. Membr. Sci.* **1994**, *95*, 147−160.
(32) Wang, Z.; Chen, T.; Xu, J. *J. Appl. Polym. Sci.* **2002**, *83*, 791−801.
(33) Wang, Z.; Chen, T.; Xu, J. *Macromolecules* **2000**, *33*, 5672−5679.
(34) Jansen, J. C.; Drioli, E. *Polym. Sci., Ser. A* **2009**, *51*, 1355−1366.
(35) García, C.; Lozano, A. E.; de la Campa, J. G.; de Abajo, J. *Macromol. Rapid Commun.* **2003**, *24*, 686−691.
(36) Zolotukhin, M. G.; Kobarbakov, V. A.; Salazkin, S. N.; Rafikov, S. R. *Vysokomol. Soedin., Ser. A* **1984**, *26*, 1212−1217.
(37) Zolotukhin, M. G.; Sedova, E. A.; Sorokina, Y. L.; Salazkin, S. N.; Sangalov, Y. A.; Sultanova, V. S.; Panasenko, A. A.; Khalilov, L. M.; Muslukhov, R. M. *Makromol. Chem.* **1990**, *191*, 1477−1485 and references therein..
(38) Bondi, A. *Physical Properties of Molecular Crystals, Liquids and Glasses*; Wiley: New York, 1968.
(39) HyperChem(TM) Professional 7.51, Hypercube, Inc., 1115 NW 4th Street, Gainesville, FL 32601.
(40) Bodor, N.; Z. Gabanyi, Z.; Wong, C. *J. Am. Chem. Soc.* **1989**, *111*, 3783−3786.
(41) Gavezotti, A. *J. Am. Chem. Soc.* **1983**, *105*, 5220−5225.
(42) Tiemblo, P.; Guzmán, J.; Riande, E.; Salvador, E. F.; Peinado, C. *J. Polym. Sci., Part B: Polym. Phys.* **2001**, *39*, 786−795. Tiemblo, P.; Guzmán, J.; Riande, E.; Mijangos, C.; Reinecke, H. *Macromolecules* **2002**, *35*, 420−424.
(43) Stejskal, E. O.; Tanner, J. E. *J. Chem. Phys.* **1965**, *42*, 288−292.
(44) Callaghan, P. T.; Jolley, K. W.; Trotter, C. M. *J. Magn. Reson.* **1980**, *39*, 525−527.
(45) Zolotukhin, M. G.; Rueda, D. R.; Balta Calleja, F. J.; Cagiao, M. E.; Bruix, M.; Sedova, E. A.; Gileva, N. G. *Polymer* **1997**, *38*, 1471−1476.
(46) Camacho-Zúñiga, C.; Ruiz-Treviño, F. A.; Zolotukhin, M. G.; del Castillo, L. F.; Guzmán, J.; Chávez, J.; Torres, G.; Gileva, G. N.; Sedova, E. A. *J. Membr. Sci.* **2006**, *283*, 393−398.
(47) Crank, J. In *The Mathematics of Diffusion*; Oxford University Press: Oxford, UK, 1975; p 51.
(48) Tiemblo, P.; Saiz, E.; Guzmán, J.; Riande, E. *Macromolecules* **2002**, *35*, 4167−4174.
(49) García, C.; López-González, M.; de Abajo, J.; Garrido, L.; Guzman, J. *Macromolecules* **2011**, *44*, 3862−3873.
(50) Vieth, W. R.; Howell, J. M.; Hsieh, J. H. *J. Membr. Sci.* **1976**, *1*, 177−220.
(51) Paul, D. R. *Ber. Bunsen-Ges.* **1979**, *83*, 294−302.
(52) Frederickson, G. H.; Helfand, E. *Macromolecules* **1985**, *18*, 2201−2207.

DOI: 10.1021/acs.macromol.5b00183
Macromolecules 2015, 48, 2585−2592